THE JOURNAL OF BIOLOGICAL CHEMISTRY VOL. 285, NO. 1, pp. 483–492, January 1, 2010

Translocation of Sphingosine Kinase 1 to the Plasma Membrane Is Mediated by Calcium- and Integrin-binding Protein 1*

Received for publication, September 21, 2009 Published, JBC Papers in Press, October 23, 2009, DOI 10.1074/jbc.M109.068395

Kate E. Jarman[‡§], Paul A. B. Moretti[‡], Julia R. Zebol[‡], and Stuart M. Pitson[‡§1]

From the [‡]Centre for Cancer Biology, SA Pathology, Frome Road, Adelaide, South Australia 5000 and [§]School of Molecular and Biomedical Science, University of Adelaide, Adelaide, South Australia 5005, Australia

SK1 (sphingosine kinase 1) plays an important role in many aspects of cellular regulation. Most notably, elevated cellular SK1 activity leads to increased cell proliferation, protection from apoptosis, and induction of neoplastic transformation. We have previously shown that translocation of SK1 from the cytoplasm to the plasma membrane is integral for oncogenesis mediated by this enzyme. The molecular mechanism mediating this translocation of SK1 has remained undefined. Here, we demonstrate a direct role for CIB1 (calcium and integrin-binding protein 1) in this process. We show that CIB1 interacts with SK1 in a Ca^{2+}-dependent manner at the previously identified "calmodulin-binding site" of SK1. We also demonstrate that CIB1 functions as a Ca^{2+}-myristoyl switch, providing a mechanism whereby it translocates SK1 to the plasma membrane. Both small interfering RNA knockdown of CIB1 and the use of a dominant-negative CIB1 we have generated prevent the agonist-dependent translocation of SK1. Furthermore, we demonstrate the requirement of CIB1-mediated translocation of SK1 in controlling cellular sphingosine 1-phosphate generation and associated anti-apoptotic signaling.

SK1 (sphingosine kinase 1) catalyzes the formation of sphingosine 1-phosphate (S1P),[2] a bioactive phospholipid that mediates a wide variety of cellular processes. Elevated cellular S1P has been shown to be pro-proliferative and anti-apoptotic (1), and considerable evidence now exists implicating SK1 in cancer. In particular, overexpression of SK1 in NIH3T3 fibroblasts leads to a transformed phenotype and the ability to form tumors in mice, with SK1 activity also involved in oncogenic H-Ras-mediated transformation (2). Furthermore, suppression of cellular SK1 activity by genetic or pharmacologic approaches has been shown to significantly reduce tumor growth *in vivo* in mice (3–5) and also sensitize tumor cells to other chemotherapeutics (6).

We have previously shown that although SK1 has intrinsic catalytic activity (7), its further activation is required for oncogenic signaling (8). This activation, brought about through phosphorylation at Ser-225 by ERK1/2, not only increases the catalytic activity of SK1 but also results in its translocation from the cytoplasm to the plasma membrane (9), which is essential for the oncogenic signaling by this enzyme (8, 10).

Although critical in understanding SK1-induced oncogenesis, the mechanisms regulating agonist-induced translocation of SK1 to the plasma membrane are poorly understood. Studies have suggested that SK1 associates with phosphatidylserine in a phosphorylation-dependent manner, providing a possible mechanism for retention of SK1 at the plasma membrane (11). Although this may facilitate retention of SK1 at the plasma membrane, the molecular mechanism mediating the initial rapid agonist-induced translocation of SK1 has not yet been established. Calmodulin (CaM) has been indirectly implicated in this process because W7, a CaM inhibitor, blocked SK1 translocation (12), as did mutation of the CaM-binding site of SK1 (13). Evidence for a direct role for CaM in SK1 translocation, however, has not been described. Furthermore, CaM predominantly moves from the cytoplasm to the nucleus, not the plasma membrane, in response to cellular Ca^{2+} fluxes (14, 15) raising doubts over the role of CaM in SK1 localization. Thus, the actual molecular mechanism mediating translocation of SK1 to the plasma membrane has remained unresolved.

In this study, we have identified the CaM-related protein CIB1 (calcium and integrin-binding protein 1) as an SK1-interacting protein. We show for the first time that CIB1 functions like a Ca^{2+}-myristoyl switch protein and is responsible for mediating the translocation of SK1 from the cytoplasm to the plasma membrane. Furthermore, we have shown that by modulating SK1 translocation, CIB1 mediates the downstream anti-apoptotic effects associated with SK1 signaling.

EXPERIMENTAL PROCEDURES

Cell Culture—Human embryonic kidney cells (HEK293T) were cultured, transfected, and harvested as described previously (16). Human cervical carcinoma (HeLa) cells were cultured and harvested in the same manner and transfected with Lipofectamine 2000 (Invitrogen). Human breast adenocarcinoma MCF7 cells were cultured in the same manner, whereas human prostate carcinoma DU145 cells were cultured in RPMI 1640 medium containing 5% fetal bovine serum.

* This work was supported by the Fay Fuller Foundation, an Australian postgraduate award, and Dawes postgraduate scholarship (to K. E. J.), Project Grant 453512, and a senior research fellowship from the National Health and Medical Research Council of Australia (to S. M. P.).

[1] To whom correspondence should be addressed. Tel.: 61-8-8222-3472; Fax: 61-8-8232-4092; E-mail: stuart.pitson@health.sa.gov.au.

[2] The abbreviations used are: S1P, sphingosine 1-phosphate; CaM, calmodulin; CHX, cycloheximide; GFP, green fluorescent protein; GST, glutathione *S*-transferase; PMA, phorbol 12-myristate 13-acetate; TNFα, tumor necrosis factor-α; HA, hemagglutinin; siRNA, small interfering RNA; PBS, phosphate-buffered saline; ERK, extracellular signal-regulated kinase.

Yeast Two-hybrid Screen—The yeast two-hybrid screen using full-length human SK1 as bait was performed as described previously (17).

Generation of CIB1 Constructs—Human CIB1 (GenBank™ accession number NM_006384) was hemagglutinin (HA) epitope-tagged at the 3′ end by *Pfu* DNA PCR with oligonucleotide primers 5′-CCCAAGCTTGCCACCATGGGGGGCTCGGGCAG-3′ and 5′-GGGGGATCCTCAAGCGTAATCTGGAACATCGTATGGGTACAGGACAATCTTAAAGGAGC-3′. The resultant product was cloned into pcDNA3 (Invitrogen) following digestion with HindIII and BamHI. The myristoylation mutant CIB1^{G2A} was generated from CIB1(HA) in pcDNA3 by QuikChange mutagenesis using the primers 5′-AGCTTGCCACCATGGCGGGATCCGGCAGTCGCCTGTCC-3′ and 5′-GGACAGGCGACTGCCGGATCCCGCCATGGTGGCAAGCT-3′.

A second nonmyristoylated CIB1 (HA-tagged at the N terminus and termed HA-CIB1) was generated by PCR using 5′-GAAGATCTTCATGGGGGGCTCGGGCAG-3′ and 5′-GGGGTACCCCTCACAGGACAATCTTAAAGGA-3′ oligonucleotide primers. The PCR product was cloned into pCMV(HA) (Clontech) following digestion with BglII and KpnI. To generate the recombinant GST-CIB1 fusion protein, CIB1 cDNA was amplified by PCR with the oligonucleotide primers 5′-CCCGGATCCGCCACCATGGGGGGCTCGGGCAG-3′ and 5′-GGGCTCGAGTCACAGGACAATCTTAAAGGA-3′, and the resultant product was cloned into pGEX4T2 (GE Healthcare) following digestion with BamHI and XhoI. Sequencing verified the integrity of all cDNAs. Mammalian expression constructs encoding human SK1, SK1^{S225A}, SK1$^{F197A/L198Q}$, and GFP-SK1 (all tagged with a C-terminal FLAG epitope) were generated as described previously (7, 9, 13).

Generation of Recombinant GST-CIB1 and Pulldown Analyses—*Escherichia coli* JM109 transformed with pGEX4T2-CIB1 plasmid was grown overnight in Luria broth containing 100 mg/liter ampicillin at 37 °C with shaking. The cultures were then diluted 1 in 10 into the same medium and grown at 37 °C for 1 h with shaking until reaching an A_{600} of ~0.6. Expression of the GST-CIB1 protein was induced by the addition of isopropyl 1-thio-β-D-galactopyranoside to a final concentration of 1 mM, and the culture was incubated for an additional 1 h. The cells were harvested by centrifugation at 6000 × *g* for 15 min at 4 °C and lysed by sonication (three 30-s pulses of 5 watts) in extraction buffer (as above) containing 1% Triton X-100. The lysate was clarified by centrifugation at 20,000 × *g* for 30 min at 4 °C to remove cell debris. GSH-Sepharose (Amersham Biosciences) was added, and the mixture was incubated at 4 °C for 1 h with constant agitation. The GSH-Sepharose beads were washed three times with cold phosphate-buffered saline (PBS), and GST-CIB1 protein remaining quantitated with Coomassie Brilliant Blue staining following SDS-PAGE using bovine serum albumin as standard. Pulldown analyses were performed by incubating 1 μg of recombinant SK1 (18) with 1 μg of the purified GST-CIB1 protein or GST alone bound to GSH-Sepharose in the presence of 2 mM $CaCl_2$, 2 mM $MgCl_2$, or 2 mM EGTA for 1 h at 4 °C with constant agitation. Inhibition of the recombinant SK1-CIB1 interaction was achieved by addition of 100 μM W7 (Calbiochem) to the mixture. Alternatively, lysates from untransfected DU145 cells or from HEK293T cells transiently transfected with the protein of interest were diluted into 33 mM Tris/HCl (pH 7.4) buffer containing 100 mM NaCl, 10% glycerol, and 0.033% Triton X-100 and incubated with the purified GST proteins under the same conditions. The GSH-Sepharose beads were pelleted by centrifugation at 3000 × *g* and washed three times in the same buffer, and bound protein was then resolved by SDS-PAGE and visualized by Western blotting. SK1, SK1^{S225A}, and SK1$^{F197A/L198Q}$ were all detected via the FLAG epitope, although recombinant SK1 was detected via its His_6 epitope.

Antibodies—M2 anti-FLAG and anti-HA antibodies were from Sigma; anti-IκBα, anti-SK1 (to immunoprecipitate endogenous SK1), and anti-His antibodies were from Santa Cruz Biotechnology (Santa Cruz, CA); anti-phospho-ERK antibodies were from Cell Signaling Technology (Danvers, MA); anti-β-tubulin antibodies were from Abcam (Cambridge, UK); and horseradish peroxidase-conjugated anti-mouse and anti-rabbit IgG were from Pierce. Anti-SK1 (for immunofluorescence) and phospho-SK1 antibodies were generated as described previously (9). Anti-CIB1 polyclonal antibodies were raised in rabbits against GST-CIB1 protein produced in *Escherichia coli* (described above) using methods previously described (9).

Affinity Purification of CIB1 Antibodies—*E. coli* cell lysate containing ~0.5 mg of GST-CIB1 was incubated with 1 ml of GSH-Sepharose for 30 min at 4 °C with constant mixing. The GSH-Sepharose and associated GST-CIB1 were then cross-linked with dimethyl pimelimidate (Pierce) as described previously (19). Rabbit anti-CIB1 serum was then applied to the resin and mixed at 4 °C for 1 h. The resin was then washed with 10 mM Tris/HCl buffer (pH 7.5) followed by 10 mM Tris/HCl buffer (pH 7.5) containing 0.5 M NaCl. The CIB1 antibody was then eluted from the resin with 100 mM glycine buffer (pH 2.5), with immediate neutralization with 1 M Tris/HCl buffer (pH 8.8). Concentration of the antibody was then achieved by precipitation through the addition of ammonium sulfate to 50% saturation at pH 7.4 and incubating the mix for 2 days at 4 °C. The precipitated antibody was pelleted by centrifugation at 20,000 × *g* for 45 min at 4 °C, and the pellet was resuspended in 1 ml of 100% saturated ammonium sulfate (pH 7.4).

Immunoprecipitation—Lysates from HEK293T cells expressing either FLAG-tagged SK1 alone or in combination with CIB1-HA in 33 mM Tris/HCl (pH 7.4) buffer containing 100 mM NaCl, 10% glycerol, 0.033% Triton X-100 and 2 mM $CaCl_2$ were incubated with anti-HA antibodies for 1 h at 4 °C with constant agitation. The immune complexes were then captured by incubation with protein A-Sepharose (GE Healthcare) for a further 1 h at 4 °C with constant agitation. Protein A-Sepharose beads were washed three times in the same buffer and then subjected to SDS-PAGE, and associated SK1 was visualized by Western blotting via the FLAG epitope. To coimmunoprecipitate the endogenous SK1-CIB1 complex, lysates from MCF7 cells in 33 mM Tris/HCl (pH 7.4) buffer containing 100 mM NaCl, 10% glycerol, 0.033% Triton X-100, and 2 mM $CaCl_2$ were incubated with anti-SK1 antibodies (Santa Cruz Biotechnology) and protein A MicroBeads (Miltenyi Biotec) for 1 h on ice. As a negative

control, a lysate sample containing no antibodies was simultaneously incubated with protein A MicroBeads. The immune complexes were captured using a 20-μm MACS® Separation Column (Miltenyi Biotec) and washed according to the manufacturer's instructions. Elution of the immune complexes was achieved through application of hot SDS-PAGE loading buffer to the column. Samples were subjected to SDS-PAGE, and the immunoprecipitated SK1 and associated CIB1 were visualized by Western blotting using anti-SK1 and anti-CIB1 antibodies, respectively.

Myristoylation of CIB1—One day after transfection, HeLa cells were incubated in Dulbecco's modified Eagle's medium containing 5% dialyzed fetal bovine serum for 2 h, and then sodium pyruvate to a final concentration of 5 mM and 0.25 mCi of [^{3}H]myristic acid (PerkinElmer Life Sciences) were added to the media, and the cells were incubated at 37 °C, 5% CO_2 for a further 5 h. Cells were harvested by scraping into cold PBS and then lysed in extraction buffer containing 1% Nonidet P-40 substitute (Sigma) by five passages through a 26-gauge needle. Lysates were incubated on ice for 30 min, and then cell debris was cleared by centrifugation at 13,000 × *g* for 20 min at 4 °C. CIB1 proteins were immunoprecipitated with anti-HA antibody and a mixture of protein A- and protein G-Sepharose as described above. The Sepharose beads were washed three times in extraction buffer containing 1% Nonidet P-40 substitute and then subjected to SDS-PAGE. The gel was fixed for 30 min in acetic acid/ethanol/water (1:4:5 by volume) followed by incubation in Amplify solution (GE Healthcare) for 1 h with agitation. The gel was then dried for 90 min at 65 °C under vacuum and exposed to film for 6 weeks at −80 °C.

Immunofluorescence—One day after transfection, HeLa cells were plated into poly-L-lysine (Sigma)-coated 8-well glass chamber slides at 10^4 cells/well and incubated for 24 h. Cells were then stimulated with 1 μg/ml phorbol 12-myristate 13-acetate (PMA; Sigma) for 30 min, 2 μM ionomycin (Calbiochem) for 2 min, or 5 μM thapsigargin (Calbiochem) for 5 min. Ca^{2+} chelation was achieved by cell treatment with 50 μM 1,2-bis(2-aminophenoxy)ethane-*N*,*N*,*N*′,*N*′-tetraacetic acid tetra(acetoxymethyl) ester (Calbiochem) for 30 min prior to stimulation with PMA. For inhibition of SK1 translocation, cells were treated with 100 μM W7 for 5 min prior to PMA stimulation. Following stimulation, cells were fixed for 10 min with 4% paraformaldehyde in PBS, permeabilized with 0.1% Triton X-100 in PBS for 10 min, and then incubated with either anti-HA or anti-SK1 antibodies in PBS containing 3% bovine serum albumin and 0.1% Triton X-100 for 1 h. The immunocomplexes were then detected with Alexa-594-conjugated anti-mouse or anti-rabbit IgG. Localization of overexpressed SK1 was visualized via its GFP fusion. Slides were mounted with Dako fluorescent mounting medium. Fluorescence microscopy was performed on an Olympus BX-51 microscope equipped with a fluorescein excitation filter (494 nm) acquired to a Cool Snap FX charge-coupled device camera (Photometrics). All images were acquired at room temperature at ×40 magnification using V++ acquisition software (Digital Optics). For quantitation of membrane localization, raw gray values were measured from eight random membrane locations per cell using Cell∧R analysis software (Olympus). Exposure times and total cell fluorescence were consistent between images used for quantitation. Mean membrane fluorescence was calculated after subtraction of background fluorescence.

siRNA Knockdown of CIB1—CIB1 siRNA oligonucleotides were purchased from Invitrogen with the following sequences: siRNA1, 5′-UAAUGGGACUUGAUGUCUGGCGUGG-3′, and siRNA2, 5′-AUGACGUGCUGGAACUCAGAGAGGU-3′. HeLa cells were transfected with either CIB1 siRNA or Validated Stealth™ negative control (Invitrogen) using HiPerFect transfection reagent (Qiagen), according to the manufacturer's protocol, and incubated for 48 h prior to harvesting and use in further experiments. All results using siRNA knockdown of CIB1 were validated by repetition with CIB1 siRNA2.

Quantitation of S1P—Cellular S1P levels were measured as described previously (16).

TNFα-induced Apoptosis—HeLa cells were treated with 2 ng/ml TNFα and 1 μg/ml cycloheximide (CHX; Sigma) for 18 h. As HeLa cells lose their adherence during programmed cell death (20), both floating (apoptotic) and live attached cells were then counted as a measure of apoptosis. To correlate floating cells with apoptotic cells, annexin V staining was performed on nonpermeabilized cells, with 99% of floating cells showing positive cell surface staining for this apoptosis marker. As a subsequent measure of apoptosis, caspase-3/7 activity was measured from cell lysates prepared from the above mentioned cells using a Caspase-Glo 3/7 assay (Promega) according to the manufacturer's protocol. The cell counts were used to standardize between samples, to give a measure of caspase-3/7 activity per cell.

NF-κB Reporter Assay—HeLa cells were transfected with either Stealth negative control or CIB1 siRNA in combination with either pIgKluc for NF-κB-dependent expression of firefly luciferase (21) or control pTK81 vector lacking the NF-κB-binding sites. pRL-TK (*Renilla* luciferase; Promega) was included in each transfection to standardize transfection efficiency. Two days following transfection, cells were stimulated with 0.5 ng/ml TNFα for 4 h, and a Dual-Luciferase reporter assay (Promega) was carried out according to the manufacturer's protocol. Firefly luminescence was standardized to *Renilla* and calculated relative to cells expressing pTK81.

RESULTS AND DISCUSSION

CIB1 Is an SK1-interacting Protein—In an attempt to identify candidate proteins that may associate with and regulate SK1, we performed a yeast two-hybrid screen. One SK1-interacting protein identified by this screen was CIB1 (also known as calmyrin and KIP (kinase-interacting protein)), a 191-amino acid Ca^{2+}-binding protein most similar in sequence to calmodulin and calcineurin B (54 and 57% amino acid sequence similarity, respectively) (22).

To initially examine the interaction between CIB1 and SK1 in mammalian cells, coimmunoprecipitation experiments were performed using cell lysates from HEK293T cells expressing FLAG-tagged SK1 and HA-tagged CIB1. The presence of SK1 in the anti-HA (CIB1) immunocomplexes supported the CIB1-SK1 interaction (Fig. 1*A*). To further confirm this interaction with endogenous SK1, bacterial expression constructs encoding glutathione *S*-transferase (GST)-CIB1 were generated. *In*

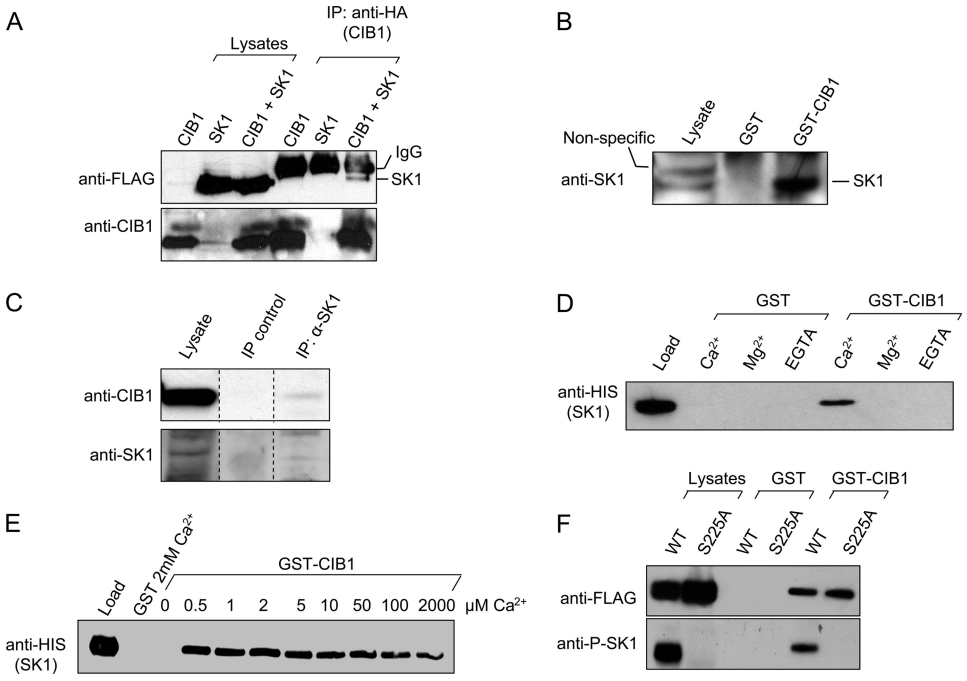

FIGURE 1. **Characterization of the CIB1-SK1 interaction.** *A*, SK1 association with CIB1 was examined by coimmunoprecipitation using lysates from HEK293T cells expressing HA-tagged CIB1 and FLAG-tagged SK1 either individually or together. Expression of these constructs was confirmed via Western blot (*lysates*). CIB1 was immunoprecipitated (*IP*) via its HA tag and associated SK1 detected by Western blot. IgG is the light chain of the anti-HA antibody used in the immunoprecipitation. *B*, recombinant GST or GST-CIB1 was incubated with cell lysates from untransfected DU145 cells (*lysate*). Endogenous SK1 pulled down by GST-CIB1 but not GST alone was detected using anti-SK1 antibodies via Western blot. *C*, to demonstrate an interaction between endogenous CIB1 and SK1, endogenous SK1 was immunoprecipitated from cell lysates of MCF7 cells (*lysate*) using anti-SK1 antibodies and protein A MicroBeads. Lysate containing protein A MicroBeads but no anti-SK1 antibodies was used as a negative control (*IP control*). CIB1 associated with the anti-SK1 immunocomplexes was detected via Western blot. Dividing lines indicate where lanes from the same Western blot have been spliced to simplify viewing. *D,* binding of SK1 to CIB1 was further examined using recombinant GST-CIB1 to bind recombinant His_6-tagged SK1 (*load*) in the presence of 2 mM $CaCl_2$, $MgCl_2$, or EGTA. *E*, Ca^{2+} concentration dependence of this interaction was determined by performing similar pulldowns with GST-CIB1 and recombinant His_6-tagged SK1 under the range of indicated $CaCl_2$ concentrations. *F*, ability of CIB1 to bind nonphosphorylated SK1 was tested using recombinant GST-CIB1 and lysates from HEK293T cells expressing either wild type (*WT*) SK1 or $SK1^{S225A}$ (*lysates*). Total SK1 was detected using anti-FLAG antibodies, whereas phospho-SK1 was detected using anti-phospho-SK1 antibodies. All data are representative of at least three independent experiments.

vitro pulldown experiments using GST-CIB1 or GST alone bound to glutathione-Sepharose, and cell lysates from DU145 cells were performed. GST-CIB1 specifically associated with endogenous SK1 from these lysates (Fig. 1*B*). To further confirm a physiologic interaction between endogenous SK1 and CIB1, coimmunoprecipitation experiments were performed from MCF7 cell lysates. Low but reproducibly detectable levels of CIB1 were present in the anti-SK1 immunocomplexes (Fig. 1*C*), demonstrating an endogenous interaction between these two proteins.

The crystal structure of CIB1 has been resolved to reveal a compact 22-kDa α-helical protein composed of closely associated globular N- and C-terminal domains, each comprising two EF-hands and separated by a flexible linker (22). This structure is similar to both CaM and calcineurin B, as well as the EF-hand containing neuronal Ca^{2+} sensor family of proteins (22). Although the two N-terminal EF-hands of CIB1 (EF-I and EF-II) do not bind metal ions, the two C-terminal EF-hands (EF-III and EF-IV) bind Ca^{2+} in a sequential manner with affinities of 1.9 and 0.5 μM, respectively (23). These values are similar to those seen with neuronal Ca^{2+} sensor proteins, enabling the binding of Ca^{2+} at concentrations just above basal levels (22). Notably, these affinities for Ca^{2+} are ~10-fold higher than those of CaM (24). Ca^{2+} binding elicits a substantial conformational change in CIB1, enabling Ca^{2+}-specific interactions with a number of its interacting proteins (23).

To investigate the Ca^{2+} dependence of the CIB1-SK1 interaction, *in vitro* pulldown experiments using GST-CIB1 or GST alone bound to GSH-Sepharose and recombinant SK1 were then performed in the presence of Ca^{2+}, Mg^{2+}, or EGTA. GST-CIB1 was only able to interact with SK1 in the presence of Ca^{2+} (Fig. 1*D*). Although preferentially binding Ca^{2+}, EF-III of CIB1 has also been described as a low affinity Mg^{2+}-binding site, with Mg^{2+} binding enabling the interaction of CIB1 with α_{IIb} integrin cytoplasmic domain peptides, albeit through a thermodynamically distinct manner (25). Mg^{2+}, however, was not able to substitute for Ca^{2+} to enable the CIB1-SK1 interaction. This was not entirely unexpected as previous NMR spectroscopy studies have revealed subtle structural differences between Mg^{2+}- and Ca^{2+}-bound CIB1, which may facilitate differential binding specificity (25). As Mg^{2+} is present in millimolar concentrations inside the cell, it has been suggested that under basal conditions, EF-III is constitutively occupied by Mg^{2+} (23, 25). Increased cytosolic Ca^{2+} levels are predicted to cause the low affinity binding of Mg^{2+} to be displaced by its higher affinity association for Ca^{2+} (23). Thus, it is likely that CIB1 interacts with SK1 only upon a rise in Ca^{2+} concentration in the cytoplasm, whereby the EF-hands of CIB1 are occupied only by Ca^{2+}.

To determine the Ca^{2+} concentration dependence of the CIB1-SK1 interaction, further *in vitro* pulldown experiments were performed using GST-CIB1 and recombinant SK1 in the presence of 0.5 μM to 2 mM $CaCl_2$. Although no interaction was observed in the absence Ca^{2+}, GST-CIB1 interacted with SK1 at values as low as 0.5 μM Ca^{2+} (Fig. 1*E*). The CIB1-SK1 interaction appeared to be strongest between 0.5 and 2 μM Ca^{2+}, which corresponds well with both physiologic cytosolic calcium concentrations (26) and the binding affinities of EF-III and EF-IV for Ca^{2+} (1.9 and 0.5 μM, respectively) (23). Thus, it is likely that at least EF-IV of CIB1 is required to be occupied by Ca^{2+} to enable the CIB1-SK1 interaction. Interestingly, at higher Ca^{2+} concentrations, particularly evident at 2 mM, the CIB1-SK1 interaction diminishes (Fig. 1*E*). This may be due to

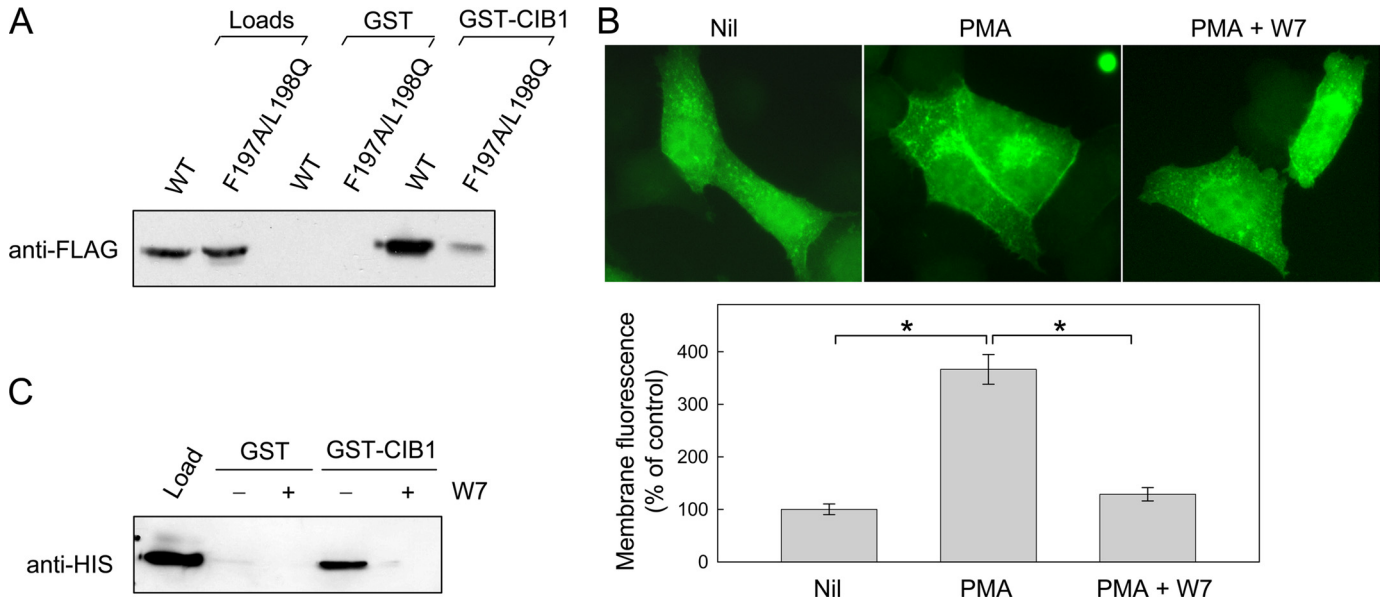

FIGURE 2. **CIB1 interacts with the CaM-binding site of SK1.** *A*, ability of CIB1 to bind SK1 mutated in the CaM-binding site was examined using recombinant GST-CIB1 and lysates from HEK293T cells expressing FLAG-tagged wild type (*WT*) SK1 or $SK1^{F197A/L198Q}$. *B*, to determine the effect of W7 on phorbol ester-induced SK1 plasma membrane translocation, HeLa cells expressing GFP-SK1 were stimulated with PMA either with or without pretreatment with W7. GFP-SK1 was visualized through fluorescence microscopy. Membrane fluorescence quantitation data represents mean ± S.E. Statistical significance was calculated by an unpaired *t* test. *, $p < 0.0001$. *C*, GST-CIB1 was used to pull down recombinant His_6-tagged SK1 in the presence or absence of 100 μM W7. All data are representative of at least three independent experiments.

the binding of Ca^{2+} into auxiliary binding sites within CIB1 at these high nonphysiologic Ca^{2+} concentrations. Notably, such binding has previously been shown to alter CIB1 structurally (27), and hence this may be responsible for the detrimental effect of high Ca^{2+} on the CIB1-SK1 interaction.

We have previously described phosphorylation of human SK1 at Ser-225, which is responsible for its activation (9) and is also critical for SK1 translocation and associated oncogenesis (8). As phosphorylation is also a well known mechanism for regulation of protein-protein interactions, we investigated whether the CIB1-SK1 interaction was also dependent upon the phosphorylation status of SK1. Pulldown analyses were performed with GST alone or GST-CIB1 bound to GSH-Sepharose with lysates from HEK293T cells expressing either wild type SK1 or $SK1^{S225A}$. GST-CIB1 was able to bind both phosphorylated and nonphosphorylated SK1 (Fig. 1*F*), suggesting this interaction is not regulated by phosphorylation of this enzyme.

CIB1 Interacts at the "CaM-binding Site" of SK1—In previous studies, we have identified the CaM-binding site in SK1 as a critical regulator of the translocation of SK1 to the plasma membrane (13). As well as sharing considerable sequence and some structural similarity, both CIB1 and CaM appear to target analogous α-helical hydrophobic regions on partner proteins (28). Given these similarities, we investigated whether the CaM-binding site on SK1 also mediates the interaction with CIB1.

Pulldown analyses were performed with GST alone or GST-CIB1 bound to GSH-Sepharose with lysates from HEK293T cells expressing either wild type SK1 or an SK1 variant containing mutations in the "CaM-binding region" ($SK1^{F197A/L198Q}$) that block its interaction with CaM (13). Mutation of the CaM-binding site of SK1 inhibited its ability to interact with CIB1, indicating that like CaM CIB1 binds to SK1 at this site (Fig. 2*A*).

The CaM inhibitor W7 has been shown to block the Ca^{2+}-associated translocation of SK1 to the plasma membrane (12). Because phorbol esters have been previously shown to induce reliable translocation of SK1 to the plasma membrane (9, 29), we examined whether W7 could also block SK1 translocation induced by this agonist. Thus, we examined the effect of W7 on localization of GFP-SK1 following cell stimulation with PMA. Although PMA induced a robust translocation of GFP-SK1 to the plasma membrane in control cells, pretreatment with W7 completely blocked this effect (Fig. 2*B*).

Although W7 is considered a CaM-specific antagonist, given the structural similarity between CIB1 and CaM and the identification that both proteins bind SK1 at the same site, we investigated whether W7 could also be an antagonist for CIB1 and inhibit the CIB1-SK1 interaction *in vitro*. Indeed, we found using pulldown analyses with GST-CIB1 bound to GSH-Sepharose and recombinant SK1 that W7 inhibited the CIB1-SK1 interaction (Fig. 2*C*). Thus, the finding that CIB1 interacts with the site on SK1 critical for its translocation, together with this inhibition of the CIB1-SK1 interaction by W7, suggested that CIB1 was a likely candidate for mediating the agonist-induced SK1 translocation.

CIB1 Acts like a Ca^{2+}-Myristoyl Switch Protein—Since its initial discovery in mediating integrin signaling by the platelet-specific integrin $\alpha_{IIb}\beta_3$ (30), CIB1 has been shown to be widely expressed in human tissues and interact with a number of other proteins. These include focal adhesion kinase (31), p21-activated kinase 1 (32), two polo-kinases Fnk and Snk (33), presenilin 2 (20), and Pax3 (34). In each of these cases, CIB1 appears to regulate quite varied signaling outcomes dependent on the target. Although the ability of CIB1 to interact with such a diverse range of proteins suggests it may have an extensive role in the regulation of cell signaling, little is known about the

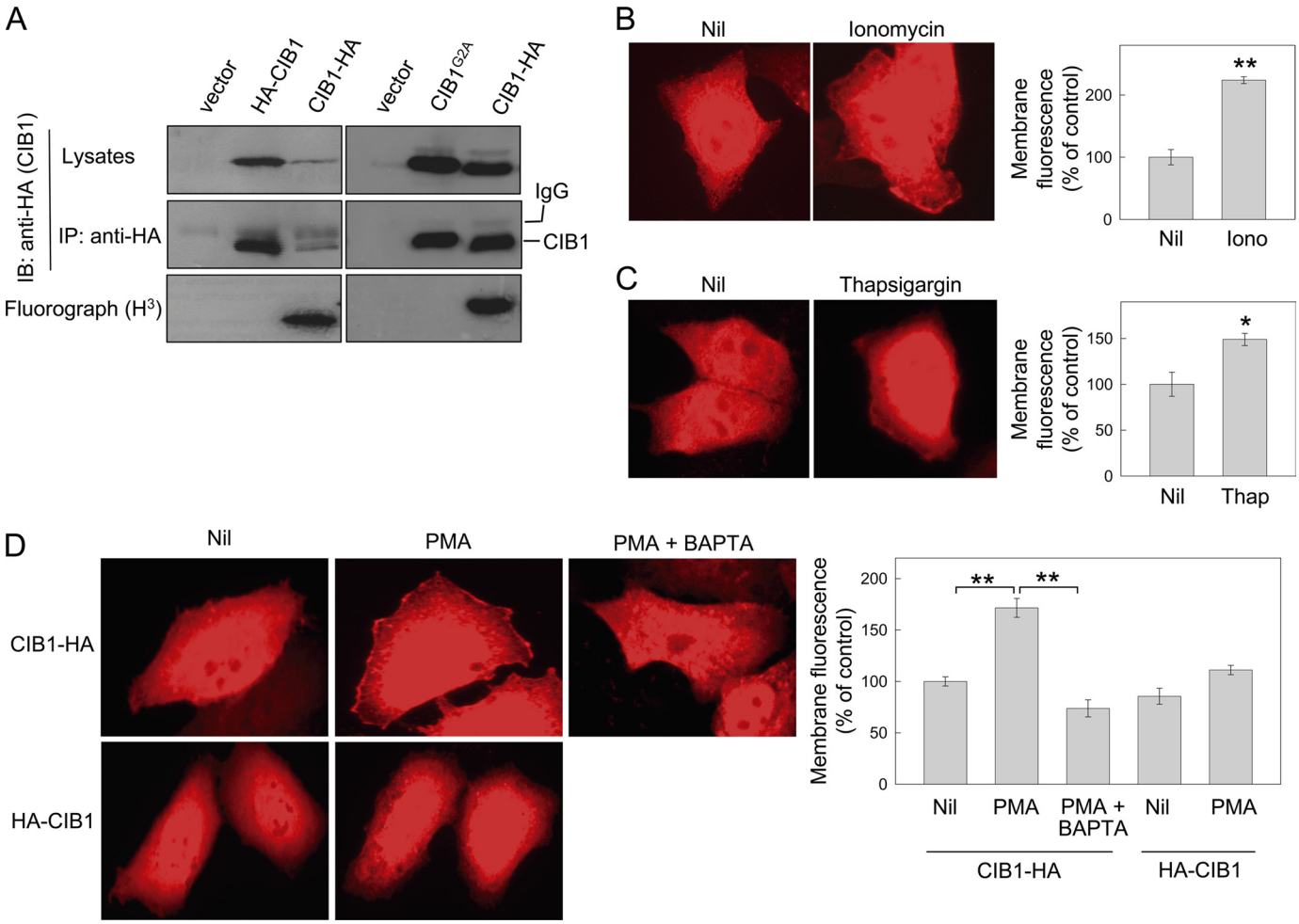

FIGURE 3. **CIB1 acts like a Ca^{2+}-myristoyl switch protein.** *A*, myristoylation status of CIB1 was determined by metabolically labeling HEK293T cells expressing CIB1 either HA-tagged at the C terminus (CIB1) or N terminus (HA-CIB1) or $CIB1^{G2A}$ (also HA-tagged at the C terminus) with [^{3}H]myristic acid. CIB1 protein was immunoprecipitated (*IP*) from these cell extracts using anti-HA antibodies, proteins separated by SDS-PAGE, and the ^{3}H signal was detected by fluorography. IgG is the light chain of the anti-HA antibody used in the immunoprecipitation. *IB,* immunoblot. *B* and *C*, fluorescence microscopy of HeLa cells expressing either CIB1 or nonmyristoylated CIB1 (HA-CIB1) detected by anti-HA antibodies following stimulation with ionomycin (*iono*) (*B*), thapsigargin (*thap*) (*C*), PMA, or 1,2-bis(2-aminophenoxy)ethane-*N*,*N*,*N*′,*N*′-tetraacetic acid/AM (*BAPTA*) and PMA (*D*). Membrane fluorescence quantitation data represent mean ± S.E. Statistical significance was calculated by an unpaired *t* test. *, $p < 0.02$; **, $p < 0.0001$.

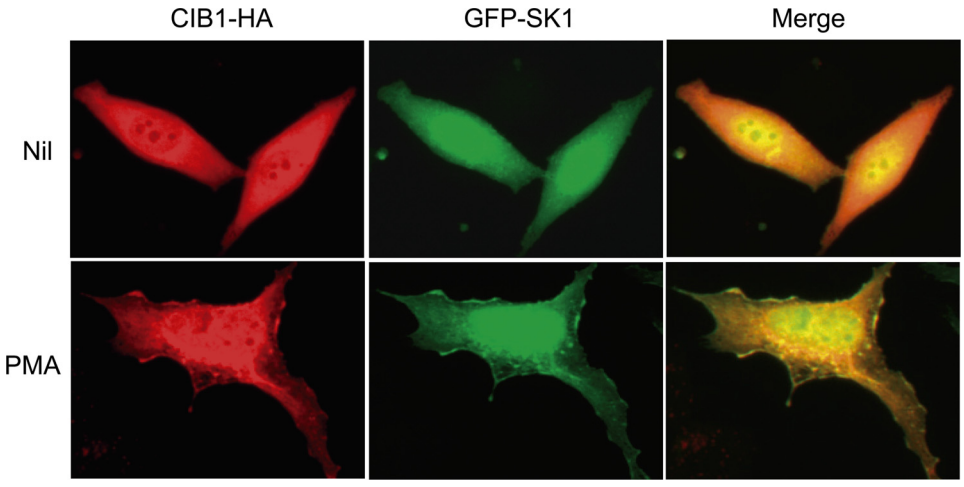

FIGURE 4. **CIB1 and SK1 colocalize at the plasma membrane following agonist stimulation.** Fluorescence microscopy of HeLa cells coexpressing CIB1 and SK1 following PMA stimulation shows colocalization of CIB1 (*red*) and SK1 (*green*) at the plasma membrane after agonist stimulation. CIB1 was detected using anti-HA antibodies, and SK1 was fused to GFP.

mechanisms by which CIB1 exerts its effects. One clue to its potential function came from a study by Stabler *et al.* (20) that showed that CIB1 is N-terminally myristoylated, leading to the hypothesis that it may act as a Ca^{2+}-myristoyl switch protein. Although this class of proteins is poorly characterized, it is generally understood that in the absence of intracellular Ca^{2+}, the myristoyl group is sequestered into a hydrophobic pocket in the protein. Binding of Ca^{2+} induces a conformational change conferring a dual effect as follows: first in enabling the interaction of the protein with target substrates, and second to cause the extrusion of the myristoyl group

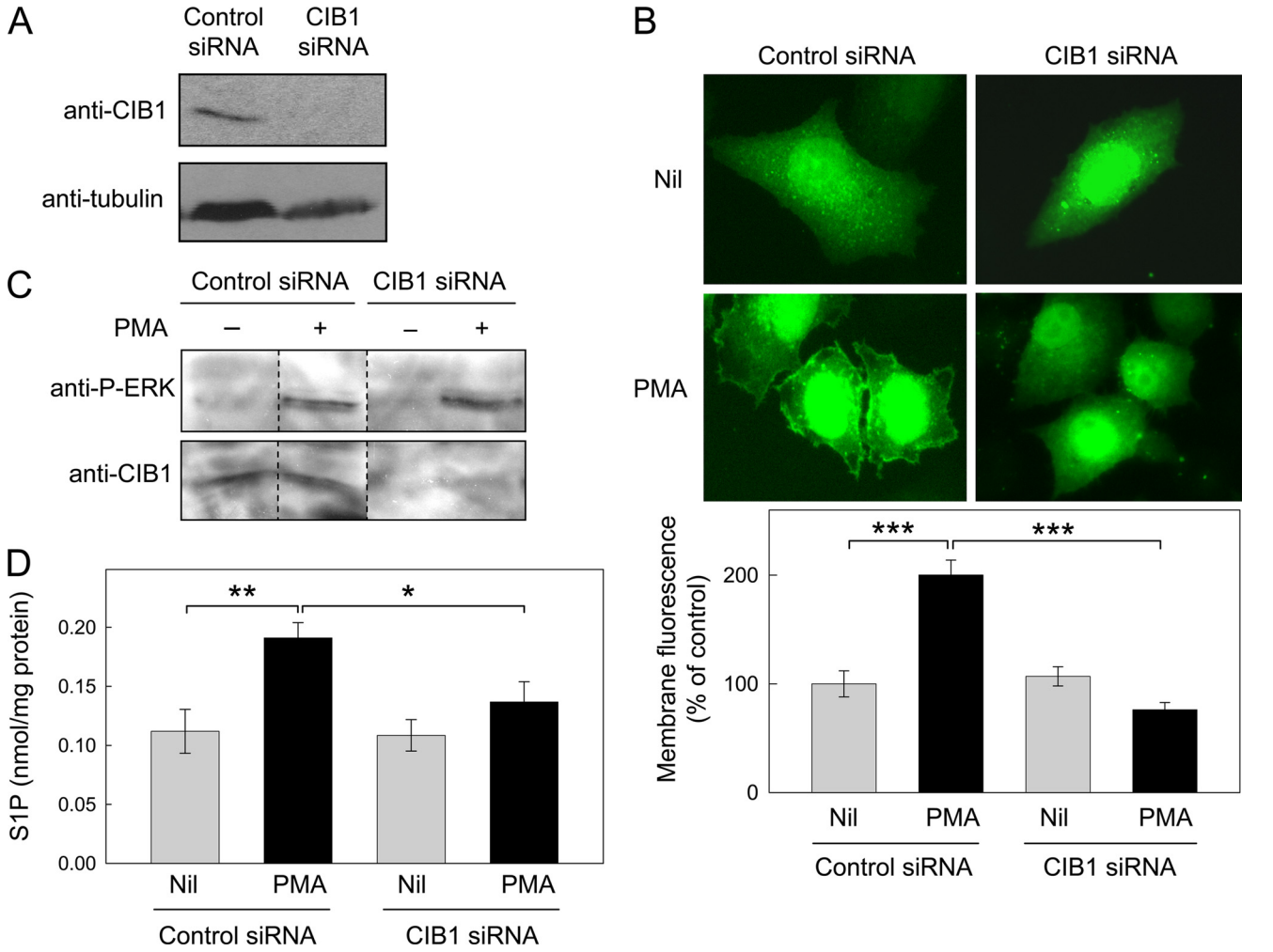

FIGURE 5. **CIB1 mediates agonist-dependent translocation of SK1 to the plasma membrane.** *A*, Western blot of HeLa cell extracts expressing GFP-SK1 and either a control siRNA (Validated Stealth™ negative control) or CIB1 siRNA demonstrating a knockdown of endogenous CIB1 protein. Tubulin levels show protein loading. *B*, fluorescence microscopy of HeLa cells coexpressing GFP-SK1 (*green*) and control siRNA or CIB1 siRNA with and without PMA stimulation. Experiments were performed with two independent CIB1 siRNAs, each generating comparable results. Membrane fluorescence quantitation data represent means ± S.E. Statistical significance was calculated by an unpaired *t* test. *C*, ERK1/2 phosphorylation was monitored in either control siRNA or CIB1 siRNA-transfected cells with or without PMA stimulation by Western blot. *Dashed lines* indicate where lanes from the same Western blot have been spliced to simplify viewing. *D*, S1P levels in either control or CIB1 siRNA transfected cells with or without PMA stimulation. Data represent the mean ± S.D. of three independent experiments, with *p* values calculated by an unpaired *t* test. ***, $p < 0.0001$; **, $p < 0.02$; and *, $p < 0.05$.

from its original sheltered groove, targeting the protein and any newly associated interacting protein to intracellular membranes (35). Hence, this hypothesis provided a potential functional mechanism by which CIB1 may traffic SK1 to the plasma membrane.

To investigate the potential function of CIB1 as a Ca^{2+}-myristoyl switch protein, we initially examined its N-terminal myristoylation. HeLa cells expressing either CIB1 (HA-tagged at the C terminus), HA-CIB1 (tagged at the N terminus to prevent any cotranslational myristoylation), or $CIB1^{G2A}$ (with its myristoylation site, Gly-2, mutated to Ala) were metabolically labeled with [^{3}H]myristic acid. Fluorography performed on CIB1 immunoprecipitated from the cell lysates demonstrated that, consistent with previous reports (20), CIB1-HA was indeed myristoylated. Addition of an N-terminal HA tag or G2A mutation prevented this myristoylation (Fig. 3*A*).

We then examined the localization of CIB1 following both an ionomycin- and thapsigargin-induced Ca^{2+} flux. Immunofluorescence performed on cells expressing CIB1 showed this protein translocates from the cytosol to the plasma membrane following ionomycin stimulation (Fig. 3*B*). Thapsigargin also induced a weak but significant plasma membrane localization of CIB1 (Fig. 3*C*). These results support the postulated function of CIB1 as a Ca^{2+}-myristoyl switch. It should be noted that these results are in contrast to a previous study that failed to observe a translocation of CIB1 to the plasma membrane upon mobilization of intracellular Ca^{2+} stores (36). This previous study, however, used a fusion protein of CIB1 with GFP, and thus the presence of GFP may have affected the localization of this protein.

We further examined the localization of CIB1 upon SK1 activation using PMA. Similar to ionomycin stimulation, PMA treatment of cells resulted in a translocation of CIB1 to the plasma membrane that could be prevented by Ca^{2+} chelation with 1,2-bis(2-aminophenoxy)ethane-*N*,*N*,*N*′,*N*′-tetraacetic acid/AM (Fig. 3*D*). This translocation was dependent upon myristoylation of the protein as no cellular relocalization was observed for the nonmyristoylated HA-CIB1. Thus, these find-

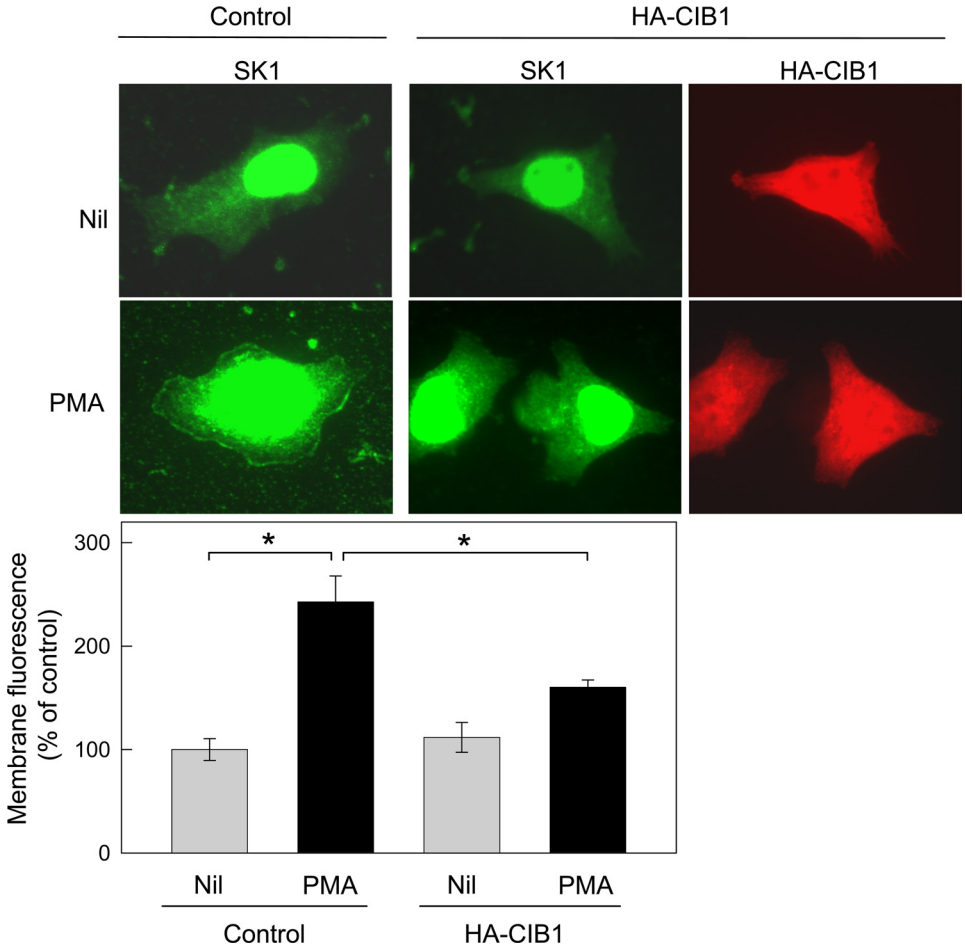

FIGURE 6. **Expression of nonmyristoylated CIB1 blocks the translocation of endogenous SK1 to the plasma membrane.** Fluorescence microscopy of either untransfected HeLa cells or cells expressing HA-CIB1 (*red*) with or without PMA stimulation. Endogenous SK1 (*green*) was detected using anti-SK1 antibodies. Membrane fluorescence quantitation data represent mean ± S.E. Statistical significance was calculated by an unpaired *t* test. *, $p < 0.002$.

ings support the Ca^{2+}-myristoyl switch function of CIB1 and represent an important mechanism by which this protein may exert its regulatory effects on target proteins.

CIB1 Mediates Translocation of SK1 to the Plasma Membrane—To investigate the role of CIB1 in translocation of SK1 to the plasma membrane, we initially examined the relative cellular localization of CIB1 and SK1 via fluorescence microscopy in cells coexpressing GFP-SK1 and CIB1. In unstimulated cells, both proteins were largely cytoplasmic, but following PMA stimulation, distinct colocalization of CIB1 and SK1 was observed at the plasma membrane (Fig. 4).

To determine the requirement of CIB1 for the agonist-driven translocation of SK1, we employed siRNA knockdown of CIB1. Following knockdown of CIB1, as monitored by the use of a CIB1 antibody (Fig. 5*A*), we examined the localization of GFP-SK1 in response to PMA stimulation. Although GFP-SK1 translocated to the plasma membrane as expected in the control cells, we saw no such relocalization of SK1 in the CIB1 knockdown cells (Fig. 5*B*), suggesting a critical requirement of CIB1 for agonist-induced translocation of SK1. Importantly, in contrast to earlier reports where CIB1 ablation reduced adhesion-induced ERK1/2 activation in endothelial cells (37), ERK1/2 activation in HeLa cells was similar in CIB1 knockdown and control siRNA cells both in unstimulated conditions and following PMA stimulation (Fig. 5*C*). Hence, the lack of SK1 translocation in CIB1-deficient cells is unlikely to result from disrupted ERK1/2 activation and supports a more direct requirement of CIB1 for SK1 translocation.

Upon activation and translocation of SK1 to the plasma membrane, cellular S1P levels increase (9). Because of the requirement of CIB1 for SK1 translocation, we investigated the effect of CIB1 knockdown on S1P levels following PMA stimulation. Although in control cells PMA stimulation induced a 2-fold increase in S1P levels, this production of S1P was attenuated in CIB1 knockdown cells (Fig. 5*D*). These results add further support to the role of CIB1 in the PMA-induced translocation of SK1 and the subsequent generation of S1P.

Expression of Nonmyristoylated CIB1 Prevents SK1 Translocation—To further confirm the requirement of CIB1 in the agonist-dependent SK1 translocation, we investigated whether expression of nonmyristoylated CIB1 could block the movement of endogenous SK1 to the plasma membrane. Cells expressing HA-CIB1 were treated with PMA, and localization of this nonmyristoylated protein as well as endogenous SK1 was observed by immunofluorescence. Untransfected cells showed a clear relocalization of endogenous SK1 to the plasma membrane upon PMA stimulation, but this was completely absent in cells expressing HA-CIB1 (Fig. 6). These results indicate that the nonmyristoylated CIB1 may act as a dominant negative to block SK1 translocation by endogenous CIB1.

Knockdown of CIB1 or Expression of Dominant-negative CIB1 Enhances Cell Susceptibility to TNFα-induced Apoptosis—SK1 activation has been shown to be critical in prevention of TNFα-induced apoptosis through NF-κB activation (38). To investigate the involvement of CIB1-mediated SK1 translocation in this process, we examined apoptosis induced by treatment with TNFα and CHX in cells where CIB1 expression was knocked down by siRNA. In comparison with control cells, a significantly increased level of apoptosis was observed in the CIB1 knockdown cells upon treatment with TNFα and CHX (Fig. 7*A*). Notably, this is consistent with previous studies that have shown embryonic fibroblasts from CIB1 knock-out mice display enhanced apoptosis compared with cells from control mice (39).

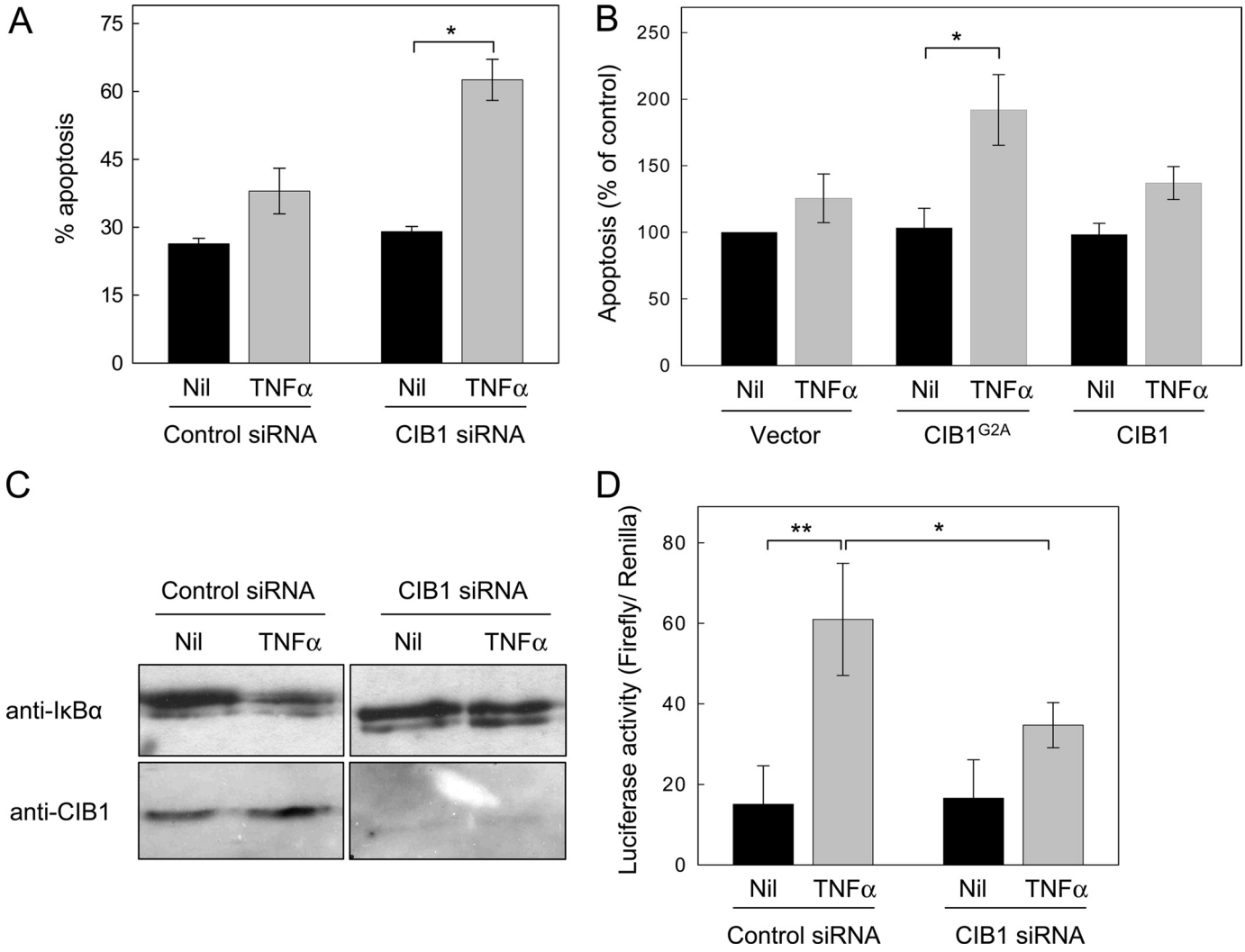

FIGURE 7. **CIB1 knockdown or use of a dominant-negative CIB1 enhances cell susceptibility to TNFα-induced apoptosis through the NF-κB pathway.** *A*, to examine the role of CIB1 in TNFα-mediated cell survival, apoptosis was measured in HeLa cells transfected with either control or CIB1 siRNA and treated with TNFα and CHX for 18 h. Apoptosis was measured through the percentage of floating cells with ~99% of these floating cells showing positive cell surface staining for the apoptosis marker annexin V. Data are the mean percentage apoptosis ± S.D. of three independent experiments. Statistical significance was calculated by an unpaired *t* test. *, $p < 0.01$. *B*, to examine whether the myristoylation of CIB1 was required for this anti-apoptotic signaling, either wild type CIB1 or nonmyristoylated CIB1^{G2A} were expressed in HeLa cells, and apoptosis was measured after TNFα and CHX for 18 h. Results show the percentage of annexin V-positive floating cells. Caspase 3/7 assays showed similar results (data not shown). Data are the mean percentage increase ± S.D. of three independent experiments calculated relative to nil-treated vector cells. Statistical significance was calculated by an unpaired *t* test. *, $p < 0.02$. *C*, HeLa cells transfected with either control or CIB1 siRNA were stimulated with TNFα for 30 min and IκB-α levels in cell lysates detected by Western blotting. *D*, HeLa cells were transfected with either control siRNA or CIB1 siRNA in combination with either pIgKluc, for NF-κB-dependent expression of firefly luciferase, or control pTK81 vector lacking the NF-κB-binding sites. pRL-TK (encoding *Renilla* luciferase) was included in each transfection to standardize transfection efficiency. Two days following transfection, cells were stimulated with 0.5 ng/ml TNFα for 4 h, and a Dual-Luciferase reporter assay was carried out. Firefly and *Renilla* luciferase activity was standardized and calculated relative to cells expressing pTK81. Data are mean ± S.D. of six independent experiments, with statistical significance calculated by an unpaired *t* test. *, $p < 0.0001$. **, $p < 0.002$.

To determine whether the myristoylation of CIB1 was required for this anti-apoptotic signaling, we also examined apoptosis induced by treatment with TNFα and CHX in cells expressing either wild type CIB1 or nonmyristoylated CIB1 (CIB1^{G2A}). These results showed that although cells expressing wild type CIB1 underwent levels of apoptosis comparable with vector-transfected cells, those expressing nonmyristoylated CIB1 had an elevated level of apoptosis after stimulation comparable with that observed in the CIB1 knockdown cells (Fig. 7*B*). These data not only highlight the necessity of myristoylation for anti-apoptotic signaling by CIB1 but also supports the dominant-negative activity of nonmyristoylated CIB1 toward SK1.

We next investigated whether this CIB1-associated anti-apoptotic signaling is mediated through NF-κB activation. CIB1 knockdown prevented NF-κB activation following TNFα stimulation, demonstrated by the degradation of IκBα (Fig. 7*C*). This was further confirmed by the use of an NF-κB reporter gene assay that showed TNFα-induced NF-κB activation was much lower in CIB1 knockdown cells compared with control cells (Fig. 7*D*). These data are consistent with previous findings that SK1 activation is essential in this process (38) and suggest that CIB1-mediated translocation of SK1 to the plasma membrane is crucial for prevention of TNFα-induced apoptosis, with this process likely mediated through NF-κB activation.

Conclusions and Implications of This Study—Localization of SK1 to the plasma membrane is crucial for mitogenic signaling by this enzyme. In this study, we have identified that CIB1 mediates the agonist-induced translocation of SK1 to the plasma membrane and thus established that CIB1 is an important regulator of SK1 function.

The identification of the Ca^{2+}-myristoyl switch function of CIB1 is the first elucidation of a mechanism by which CIB1 may mediate its regulatory effects on its various target proteins in cells. We propose a model whereby under basal conditions the EF-hands of CIB1 are bound by Mg^{2+}, preventing the interaction of CIB1 with SK1. Upon activation of SK1, increases in cytosolic Ca^{2+} concentration have been widely observed (40), and this would first enable CIB1 to interact with SK1 but also result in the translocation of CIB1 and newly bound SK1 to the plasma membrane. Notably, CIB1 binds to both phosphorylated and nonphosphorylated SK1 despite the observation that nonphosphorylated SK1 does not appear to localize to the plasma membrane. However, as phosphorylated SK1 has been reported to preferentially bind phosphatidylserine (11), it is likely that only phosphorylated SK1 is retained at the plasma membrane via association with this phospholipid.

The ability of CIB1 to mediate S1P generation and SK1-associated anti-apoptosis illustrates the importance of CIB1 in the biologic role of SK1. In addition to this anti-apoptotic role, CIB1 has also been shown to mediate cell proliferation, with knockdown of CIB1 reducing proliferation in both mouse heart and lung endothelial cells (37). Again, this is consistent with the pro-proliferative effect of SK1 activation and translocation in cells. Together, these findings suggest CIB1 to be an important mediator of at least some of the biologic effects of SK1 activation, and consequently, CIB1 may represent a promising target for modulating SK1 signaling in cells.

REFERENCES

1. Olivera, A., Kohama, T., Edsall, L., Nava, V., Cuvillier, O., Poulton, S., and Spiegel, S. (1999) *J. Cell Biol.* **147,** 545–558
2. Xia, P., Gamble, J. R., Wang, L., Pitson, S. M., Moretti, P. A., Wattenberg, B. W., D'Andrea, R. J., and Vadas, M. A. (2000) *Curr. Biol.* **10,** 1527–1530
3. French, K. J., Schrecengost, R. S., Lee, B. D., Zhuang, Y., Smith, S. N., Eberly, J. L., Yun, J. K., and Smith, C. D. (2003) *Cancer Res.* **63,** 5962–5969
4. Kohno, M., Momoi, M., Oo, M. L., Paik, J. H., Lee, Y. M., Venkataraman, K., Ai, Y., Ristimaki, A. P., Fyrst, H., Sano, H., Rosenberg, D., Saba, J. D., Proia, R. L., and Hla, T. (2006) *Mol. Cell. Biol.* **26,** 7211–7223
5. Kawamori, T., Kaneshiro, T., Okumura, M., Maalouf, S., Uflacker, A., Bielawski, J., Hannun, Y. A., and Obeid, L. M. (2009) *FASEB J.* **23,** 405–414
6. Pchejetski, D., Golzio, M., Bonhoure, E., Calvet, C., Doumerc, N., Garcia, V., Mazerolles, C., Rischmann, P., Teissié, J., Malavaud, B., and Cuvillier, O. (2005) *Cancer Res.* **65,** 11667–11675
7. Pitson, S. M., D'andrea, R. J., Vandeleur, L., Moretti, P. A., Xia, P., Gamble, J. R., Vadas, M. A., and Wattenberg, B. W. (2000) *Biochem. J.* **350,** 429–441
8. Pitson, S. M., Xia, P., Leclercq, T. M., Moretti, P. A., Zebol, J. R., Lynn, H. E., Wattenberg, B. W., and Vadas, M. A. (2005) *J. Exp. Med.* **201,** 49–54
9. Pitson, S. M., Moretti, P. A., Zebol, J. R., Lynn, H. E., Xia, P., Vadas, M. A., and Wattenberg, B. W. (2003) *EMBO J.* **22,** 5491–5500
10. Wattenberg, B. W., Pitson, S. M., and Raben, D. M. (2006) *J. Lipid Res.* **47,** 1128–1139
11. Stahelin, R. V., Hwang, J. H., Kim, J. H., Park, Z. Y., Johnson, K. R., Obeid, L. M., and Cho, W. (2005) *J. Biol. Chem.* **280,** 43030–43038
12. Young, K. W., Willets, J. M., Parkinson, M. J., Bartlett, P., Spiegel, S., Nahorski, S. R., and Challiss, R. A. (2003) *Cell Calcium* **33,** 119–128
13. Sutherland, C. M., Moretti, P. A., Hewitt, N. M., Bagley, C. J., Vadas, M. A., and Pitson, S. M. (2006) *J. Biol. Chem.* **281,** 11693–11701
14. Chin, D., and Means, A. R. (2000) *Trends Cell Biol.* **10,** 322–328
15. Thorogate, R., and Török, K. (2007) *Biochem. J.* **402,** 71–80
16. Leclercq, T. M., Moretti, P. A., Vadas, M. A., and Pitson, S. M. (2008) *J. Biol. Chem.* **283,** 9606–9614
17. Zebol, J. R., Hewitt, N. M., Moretti, P. A., Lynn, H. E., Lake, J. A., Li, P., Vadas, M. A., Wattenberg, B. W., and Pitson, S. M. (2009) *Int. J. Biochem. Cell Biol.* **41,** 822–827
18. Pitson, S. M., Moretti, P. A., Zebol, J. R., Zareie, R., Derian, C. K., Darrow, A. L., Qi, J., D'Andrea, R. J., Bagley, C. J., Vadas, M. A., and Wattenberg, B. W. (2002) *J. Biol. Chem.* **277,** 49545–49553
19. Bar-Peled, M., and Raikhel, N. V. (1996) *Anal. Biochem.* **241,** 140–142
20. Stabler, S. M., Ostrowski, L. L., Janicki, S. M., and Monteiro, M. J. (1999) *J. Cell Biol.* **145,** 1277–1292
21. Himes, S. R., Coles, L. S., Reeves, R., and Shannon, M. F. (1996) *Immunity* **5,** 479–489
22. Gentry, H. R., Singer, A. U., Betts, L., Yang, C., Ferrara, J. D., Sondek, J., and Parise, L. V. (2005) *J. Biol. Chem.* **280,** 8407–8415
23. Yamniuk, A. P., Nguyen, L. T., Hoang, T. T., and Vogel, H. J. (2004) *Biochemistry* **43,** 2558–2568
24. Burgoyne, R. D., and Weiss, J. L. (2001) *Biochem. J.* **353,** 1–12
25. Yamniuk, A. P., and Vogel, H. J. (2005) *Protein Sci.* **14,** 1429–1437
26. Berridge, M. J., Lipp, P., and Bootman, M. D. (2000) *Nat. Rev. Mol. Cell Biol.* **1,** 11–21
27. Yamniuk, A. P., Anderson, K. L., Fraser, M. E., and Vogel, H. J. (2009) *Protein Sci.* **18,** 1128–1134
28. Barry, W. T., Boudignon-Proudhon, C., Shock, D. D., McFadden, A., Weiss, J. M., Sondek, J., and Parise, L. V. (2002) *J. Biol. Chem.* **277,** 28877–28883
29. Johnson, K. R., Becker, K. P., Facchinetti, M. M., Hannun, Y. A., and Obeid, L. M. (2002) *J. Biol. Chem.* **277,** 35257–35262
30. Naik, U. P., and Naik, M. U. (2003) *Blood* **102,** 1355–1362
31. Naik, M. U., and Naik, U. P. (2003) *Blood* **102,** 3629–3636
32. Leisner, T. M., Liu, M., Jaffer, Z. M., Chernoff, J., and Parise, L. V. (2005) *J. Cell Biol.* **170,** 465–476
33. Kauselmann, G., Weiler, M., Wulff, P., Jessberger, S., Konietzko, U., Scafidi, J., Staubli, U., Bereiter-Hahn, J., Strebhardt, K., and Kuhl, D. (1999) *EMBO J.* **18,** 5528–5539
34. Hollenbach, A. D., McPherson, C. J., Lagutina, I., and Grosveld, G. (2002) *Biochim. Biophys. Acta* **1574,** 321–328
35. Ames, J. B., Ishima, R., Tanaka, T., Gordon, J. I., Stryer, L., and Ikura, M. (1997) *Nature* **389,** 198–202
36. Blazejczyk, M., Wojda, U., Sobczak, A., Spilker, C., Bernstein, H. G., Gundelfinger, E. D., Kreutz, M. R., and Kuznicki, J. (2006) *Biochim. Biophys. Acta* **1762,** 66–72
37. Zayed, M. A., Yuan, W., Leisner, T. M., Chalothorn, D., McFadden, A. W., Schaller, M. D., Hartnett, M. E., Faber, J. E., and Parise, L. V. (2007) *Circ. Res.* **101,** 1185–1193
38. Xia, P., Wang, L., Moretti, P. A., Albanese, N., Chai, F., Pitson, S. M., D'Andrea, R. J., Gamble, J. R., and Vadas, M. A. (2002) *J. Biol. Chem.* **277,** 7996–8003
39. Yuan, W., Leisner, T. M., McFadden, A. W., Clark, S., Hiller, S., Maeda, N., O'Brien, D. A., and Parise, L. V. (2006) *Mol. Cell. Biol.* **26,** 8507–8514
40. Spiegel, S., and Milstien, S. (2003) *Nat. Rev. Mol. Cell Biol.* **4,** 397–407